







Rare Holocene sediment deposits from Sodmein Playa (Eastern Desert, Egypt)—Stratigraphic assessment and environmental setting

Felix Henselowsky^{1,2,3}  | Nicole Klasen^{3,4} | Rhys Timms^{5,6}  | Dustin White^{5,7} | Paul Lincoln^{5,6}  | Simon Blockley⁵  | Karin Kindermann^{3,8}  | Olaf Bubbenzer^{2,3} 

¹Institute of Geography, Johannes Gutenberg University Mainz, Mainz, Germany

²Institute of Geography, Heidelberg University, Heidelberg, Germany

³Collaborative Research Centre 806 “Our Way to Europe”, University of Cologne, Cologne, Germany

⁴Institute for Geography, University of Cologne, Cologne, Germany

⁵Department of Geography, Centre for Quaternary Research, Royal Holloway University of London, Surrey, UK

⁶School of Archaeology, Geography and Environmental Science, University of Reading, Reading, UK

⁷Department of Chemistry, University of York, York, UK

⁸Institute of Prehistoric Archaeology, University of Cologne, Cologne, Germany

Correspondence

Felix Henselowsky, Institute of Geography, Johannes Gutenberg University Mainz, Johann-Joachim-Becher-Weg 21, 55099 Mainz, Germany.

Email: felix.henselowsky@uni-mainz.de

Scientific editing by Kevin Walsh.

Funding information

Deutsche Forschungsgemeinschaft

Abstract

Sodmein Playa is one of the rare Pleistocene open-air sites in the Eastern Desert of Egypt. Based on the associated stone artefact material, it could be assigned to the Middle Stone Age/Last Interglacial. However, it has not yet been possible to clarify whether the sediments at the basin originated during the Pleistocene or later during Holocene wet phases. Our integrative approach combining Optically Stimulated Luminescence chronology, and cryptotephra analysis, allows us to link the environmental archive of Sodmein Playa with the site of Sodmein Cave. Sodmein Playa indicates wetter climate conditions starting around 9 ka with a (relative) maximum around 7 ka, in line with the general framework of the Holocene Humid Period in Northeast Africa. Despite the climatic similarity, regional environmental differences can still be identified and the effective available water around Sodmein Playa is reduced. The results are well integrated into the current archaeological knowledge with the change from hunter-gatherers to herders during the Holocene in the area. Analyses of cryptotephra reveal a wide range of source regions, including Eastern and Central Anatolian, the Azores, and the Aegean, as well as those which remain uncorrelated. A tentative correlation with the Holocene cryptotephra record from Sodmein Cave is established.

KEYWORDS

Cryptotephra, Northeast Africa, OSL, Playa

This is an open access article under the terms of the Creative Commons Attribution License, which permits use, distribution and reproduction in any medium, provided the original work is properly cited.

© 2022 The Authors. *Geoarchaeology* published by Wiley Periodicals LLC.

1 | INTRODUCTION

In the past decades, important archaeological sites were discovered in the Eastern Desert of Egypt, within the Gebel Duwi mountain ridge area. Sodmein Cave and Tree Shelter have given evidence of human occupation during the Late Pleistocene and Holocene. These sites are valuable for helping to understand both the Pleistocene dispersal of humans and the first appearance of domesticated animals during the early to mid-Holocene in Northeast Africa (cf. Marinova et al., 2008; Schmidt et al., 2015; Van Peer et al., 1996; Vermeersch et al., 2015). The eroding landscape and the present-day hyperarid environment, in which these sites are located, however, are challenging for answering questions with regard to stratigraphies and palaeoenvironmental conditions. It can be assumed that none of the geo- and archaeological archives in the Eastern Desert can provide comprehensive insights and that the information on human–environment relations is only available as a complex mosaic. Ultimately, this is also due to the fact that there is a very close interaction of different geomorphological units in desert environments, on a regional to local scale: geologically old, stable surfaces lie close to each other to significantly younger and recently active ones. A full comprehensive stratigraphic archive is usually not available at a particular location but is achievable from the integration of spatially differentiated evidence.

Geoarchaeological research during the Collaborative Research Centre 'Our Way to Europe' (CRC 806; Litt et al., 2021; Richter et al., 2012) tried to overcome this issue with extensive surveys. This led to the discovery of the open-air site Sodmein Playa, which can be attributed to the presence of specific stone artefacts from the Early Nubian Complex (Last Interglacial) (Kindermann et al., 2018). However, the stratigraphic assessment and the subsequent sedimentological analysis of the central infilled basin, adjacent to the archaeological site, have not been reported yet.

Initial hypotheses assumed that an ephemeral lake formed during wetter climate phases, such as during the Last Interglacial (Kindermann et al., 2018) or even later, during the Early Holocene, when people started to reoccupy the area following their absence during the Last Glacial Maximum (Vermeersch et al., 2015). However, since the initial investigations could neither reach the base of the infilling nor determine the time for individual sediment phases, a reliable chronological framework for the basin is lacking. Here, we report optically stimulated luminescence (OSL) dating and grain-size analyses to gather insights into the depositional environment and to refine the first qualitative interpretation of the stratigraphy in the depression. In addition, the results of a cryptotephra analysis throughout the sediment sequence provide a correlation and a stratigraphic linkage of the playa stratigraphy with those of Sodmein Cave, where two distinct cryptotephra layers could be distinguished and analysed from the Pleistocene and Holocene deposits (Barton et al., 2015).

2 | SITE DESCRIPTION

Sodmein Playa (33° 56' E, 26°13' N) is located in the western part of the Gebel Duwi mountain ridge between small outcrops of Nubian Sandstone, about 3 km from Sodmein Cave (Figure 1). Here, a wadi terrace bar is elevated up to 2 m above the present wadi floor, presenting a marked cuesta-like profile as a consequence of a posterior wadi incision (Kindermann et al., 2018). The wadi is part of a larger fluvial system that drains towards the Red Sea (Yousif et al., 2018). Behind the named terrace remnant, which acts as a kind of barrier, a low and flat area is situated. The surface of this small basin consists of sand and fine gravels. This central depression of the Sodmein Playa covers an area of about 12,000 m². The surface gently slopes up to the southwest, extending between low outcrops of Nubian Sandstone towards the southwestern extension. Profile 5, located in the central part of the depression, comprises a thick sequence with fine sediments underneath the surface. The stratigraphy was first described based on field observations, with an initial interpretation of the different sedimentological and stratigraphic units by Kindermann et al. (2018).

Today, the region has a hyperarid desert climate. The modern climate, based on data from the closest WMO weather station, shows total annual precipitation of less than 20 mm on average, with erratic rainfall events in the winter months and very high evaporation rates. The annual temperature is 24.2°C, with the average temperature being lowest in January (17.8°C) and highest in August (29.9°C) (WMO-station 62465-Quesir, UN data).

3 | METHODS

Sampling for sedimentology and OSL dating was undertaken in 2017 for subsequent analysis at the laboratory of the Institute for Geography and the Cologne Luminescence Laboratory (both University of Cologne). A 1.5 m deep trench from preliminary investigations in 2014 was reinvestigated. Hand auger drilling attempted to reach a greater depth but was stopped at 1.9 m due to technical limitations of the equipment. Sediment samples from each sedimentological unit were taken from profile P5 located in the central part of the Sodmein Playa depression (Figure 1d). Four OSL samples (1401-P1 to 1401-P4) were taken after cleaning the profile. They were collected in opaque plastic tubes to prevent contact with daylight. The surrounding material of each sample was collected to measure the radionuclide activity with high-resolution gamma-ray spectrometry in the laboratory. Sampling for tephra analysis was carried out at systematic intervals of 5 cm.

3.1 | OSL

Sample preparation (removal of carbonates, organics, clay and density separation for quartz) followed standard procedures (comp. e.g., Klasen et al., 2018). The single-aliquot regenerative-dose protocol

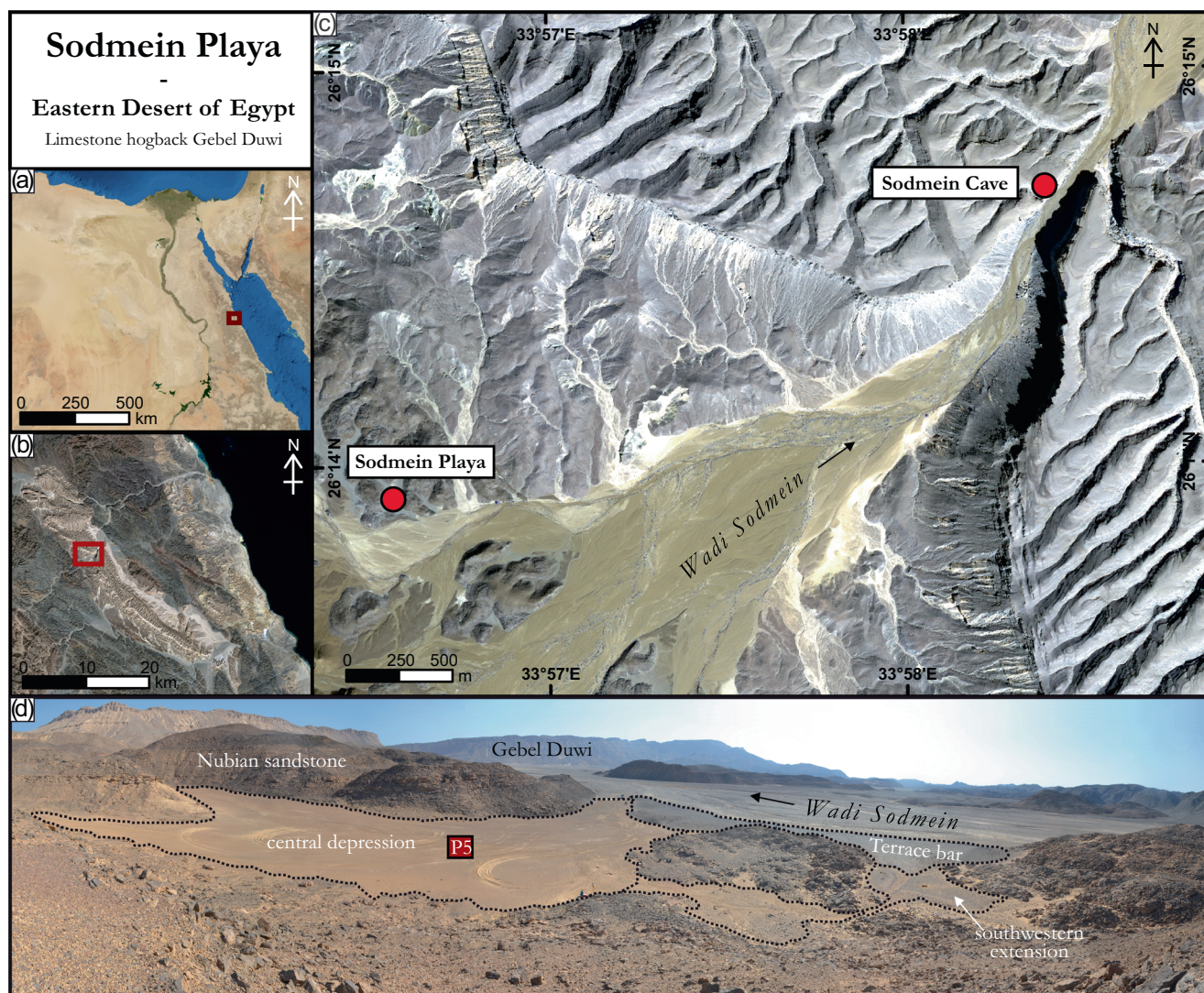


FIGURE 1 Site location of Sodmein Playa; (a) in the Eastern Desert of Egypt (Modis satellite image); (b) at the central limestone ridge of the Gebel Duwi (Landsat-8, (US Geological Survey products, bands 234) and (c) in correlation with Wadi Sodmein and Sodmein Cave (QuickBird Satellite image, bands 432). (d) Panoramic image of the area.

(SAR, Murray & Wintle, 2000, 2003) was applied to date quartz samples derived from the 150–200 μm grain-size fraction. Measurements were carried out with an automated Risø TL/OSL DA 20 reader equipped with a calibrated ^{90}Sr beta source. Blue-light emitting diodes (470 nm, FWHM = 20 nm) and Hoya U 340 filter (7.5 mm) transmitting wavelengths of 330 ± 40 nm were used for optical stimulation and signal detection of the quartz multigrain aliquots (8 mm diameter of the grain layer). The net OSL signal was obtained using the first 0.5 s of the stimulation and early background subtraction of the subsequent 1.3 s (Ballarini et al., 2007; Cunningham & Wallinga, 2010). The response to IR stimulation was measured at the end of the SAR cycle (Duller, 2003). For a preheat plateau test, we employed preheat temperatures between 180°C and 280°C for 10 s, a cut heat temperature of 20°C below the preheat temperature, and OSL stimulation for 40 s at 125°C (8 mm, three aliquots each temperature). Additionally, we carried out dose recovery tests of the same samples (given dose: 15 Gy (1401P1-1)

and 19 Gy (1401P1-2, P1-3, P1-4) after OSL stimulation for 100 s at room temperature) using a preheat temperature of 240°C and a cut heat temperature of 220°C (8 mm, five aliquots). The radionuclide activity of the surrounding sediments was measured using high-resolution gamma-ray spectrometry. The dose rate was calculated using the Dose Rate and Age Calculator (DRAC, Durcan et al., 2015) and the included conversion factors of Guerin et al. (2011), attenuation factors of Brennan et al. (1991) and Brennan (2003), an a -value of 0.04 ± 0.03 , and an assumed water content of $5 \pm 2\%$. The cosmic dose rate was calculated following Prescott and Hutton (1994).

3.2 | Grain-size distribution

Grain-size analyses were done by laser diffraction using a Beckmann Coulter LS 13320. It can detect the particle size

between 2000 and 0.04 μm and provide 126 distinct classes for the grain-size distribution. All samples were treated with hydrogen peroxide (H₂O₂ 15%) to remove organic matter. Before measurement, the samples were treated with sodium pyrophosphate (Na₄O₇P₂, 46 g/l) to avoid any flocculation. Duplicate sample sets were measured with and without HCl (10%) pretreatment to remove carbonates. The excel spreadsheet GRADISTAT (Version 8.0) (Blott & Pye, 2001) was used to investigate the grain-size distribution statistics.

3.3 | Cryptotephra analyses

Samples for cryptotephra analyses were heated to 550°C for 2 h to remove detrital organic content, followed by immersion in 10% HCl to remove carbonates. Each sample was wet sieved at 80 and 15 μm with the intermediary fraction retained before glass shard extraction was undertaken following the protocols of Blockley et al. (2005). Three intervals determined to have the highest glass shard concentrations (SOD 0–5, 5–10 and 40–45) were prepared from Sodmein Playa for major element chemical analysis.

Samples selected for geochemical analyses were re-extracted but without using the 550°C heating step to avoid chemical alteration of the tephra. Individual glass shards were then extracted from the host substrate using a micromanipulator fitted with a 5 μl gas chromatography syringe and a 100 μm diameter needle. These glass shards were transferred to a flat silicon sheet and impregnated in an epoxy resin. Once hardened, the silicon sheet was removed and the resin block or ‘stub’ was gradually cut down using silicon grinding papers to expose the glass shards at the surface. A final polish using 0.3 μm aluminium oxide powder provided a flat clean surface for analysis. Sectioned stubs were sent to the Tephra Analysis Unit (TAU) at the University of Edinburgh, where they were carbon-coated and analysed for major elements using a WDS-EPMA (Cameca SX-100). Probe conditions followed Hayward (2012).

4 | RESULTS

The results of the grain-size distribution analysis verify the field observations that the proportion of gravel, sand and silt varies throughout the stratigraphy (Figure 2). The lowermost part of the

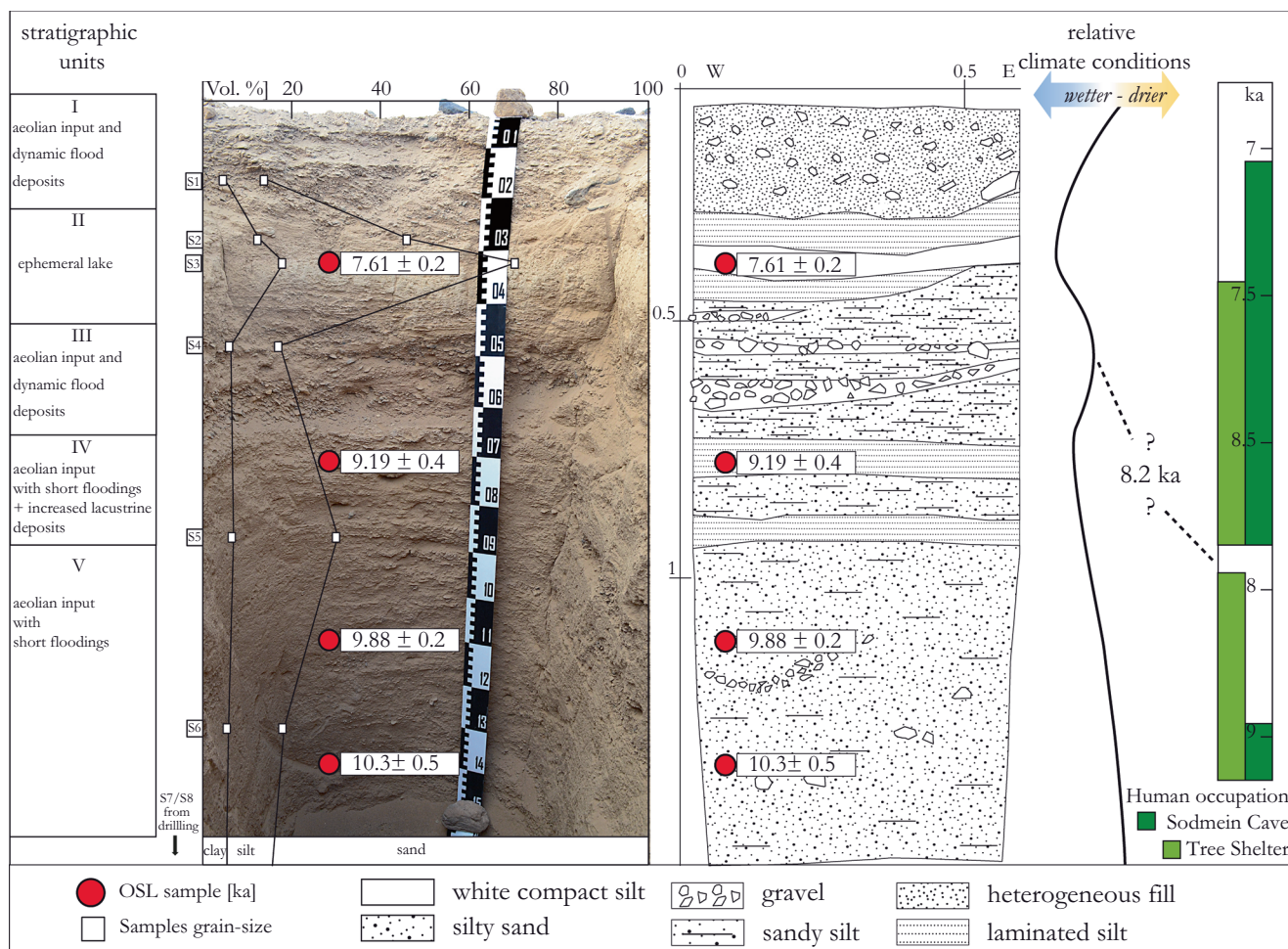


FIGURE 2 Chronology and environmental implications from Sodmein Playa. Sediment stratigraphy central Sodmein Playa, Profile 5; Profile Sketch after Kindermann et al. (2018); phases of human occupation at Sodmein Cave and Tree Shelter after Vermeersch et al. (2015).

TABLE 1 Results of optically stimulated luminescence measurements and calculated ages

Sample ID	Sample name	Sampling depth (m b.s.)	Water content (%)	Accepted/measured aliquots (n)	Radionuclide concentration					RSD (%)	De (Gy)	Age (ka)
					U (ppm)	Th (ppm)	K (%)	Dose rate (Gy/ka)				
C-L4479	1401 P1-1	0.35	5 ± 2	49/49	2.50 ± 0.12	8.59 ± 0.43	0.80 ± 0.02	1.96 ± 0.04	13	14.9 ± 0.27	7.61 ± 0.20	
C-L4480	1401 P1-2	0.8	5 ± 2	31/32	2.43 ± 0.11	8.79 ± 0.44	0.61 ± 0.01	1.74 ± 0.03	23	16.0 ± 0.66	9.19 ± 0.42	
C-L4481	1401 P1-3	1.2	5 ± 2	33/33	1.89 ± 0.09	6.30 ± 0.33	0.61 ± 0.01	1.45 ± 0.03	9	14.3 ± 0.24	9.88 ± 0.23	
C-L4482	1401 P1-4	1.45	5 ± 2	41/42	2.71 ± 0.10	7.51 ± 0.38	0.57 ± 0.01	1.68 ± 0.03	28	17.3 ± 0.76	10.3 ± 0.49	

sequence consists of a thick, predominantly fine sandy unit (S8). Within these sands, very fine silty laminae and fine gravels occur. Medium and coarse sand is enhanced in the overlying part of the profile, where also a few gravel >2 mm occur (S7). The grain-size distribution from S7 to S5 shows a slight increase in the amount of silt and a more widespread grain-size distribution. The silt fraction increases between S7 (9.5%) and S5 (23.4%). This is in accordance with field observations and an increase in laminae of silt particles between 70 and 90 cm. The trend towards more silty sediments is interrupted with one layer of coarse-grained materials, predominantly fine and medium sand including coarse sand and fine gravel (S4). This unit is capped with thick and homogeneous white silts with a very compact texture, which strongly reacts to HCl treatment due to the carbonates. However, it cannot be ruled out that gypsum/anhydrite or other evaporites also occur. Here, the maximum amount of silt within the stratigraphy is present at 52.4% (S3), followed by a small decrease towards 33.6% (S2). Whereas all layers have a clay content between 4.6% and 6.6%, clay content has also its maximum with 17.9% (S3) and 12.3% (S2) in this layer. The uppermost layer is of heterogeneous materials with mixed gravels, sand and only a limited amount of silt (20.5%).

Differences between the grain-size distribution with and without HCl are very low for all samples, excluding S2, indicating a shift in the medium sand fraction towards fine sand after carbonate dissolution.

4.1 | Chronology

The chronology of the deposits based on OSL dating (Table 1) starts at 10.3 ± 0.5 ka (PL4) at the base of the sediment profile. A relative rapid sediment accumulation is observed in the lower part of the sequence, as the ages between 140 and 80 cm (PL4 10.3 ± 0.5 ka; PL3 9.88 ± 0.2 ka; and PL2 9.19 ± 0.4 ka) are very close to each other and partly overlap within the measurement uncertainty. The youngest age is obtained for the fine-grained deposits, dated to 7.61 ± 0.2 ka (0.35 cm, PL1).

4.2 | Cryptotephra

Seven cryptotephra analyses were carried out on samples from SOD 40–45, eight analyses from SOD 5–10, and 28 analyses from SOD 0–5. Three of the seven analyses characterizing SOD 40–45 exhibit analytical totals below 95 wt.% and are thus excluded from further interpretation (Hunt & Hill, 1993). The remaining four analyses from SOD 40–45 form a single chemical population that can be classified as rhyolite (Figure 3a; comp. BAS et al., 1986). The eight analyses composing SOD 5–10 can be grouped into three populations and are all classified as rhyolites (Figure 3a; comp. BAS et al., 1986). Four of the 28 analyses obtained from SOD 0–5 were excluded from further interpretation due to low analytical totals (<95 wt.%). Of the remaining 23 analyses, eight chemical populations can be potentially recognized. Six of the populations can be classified broadly as

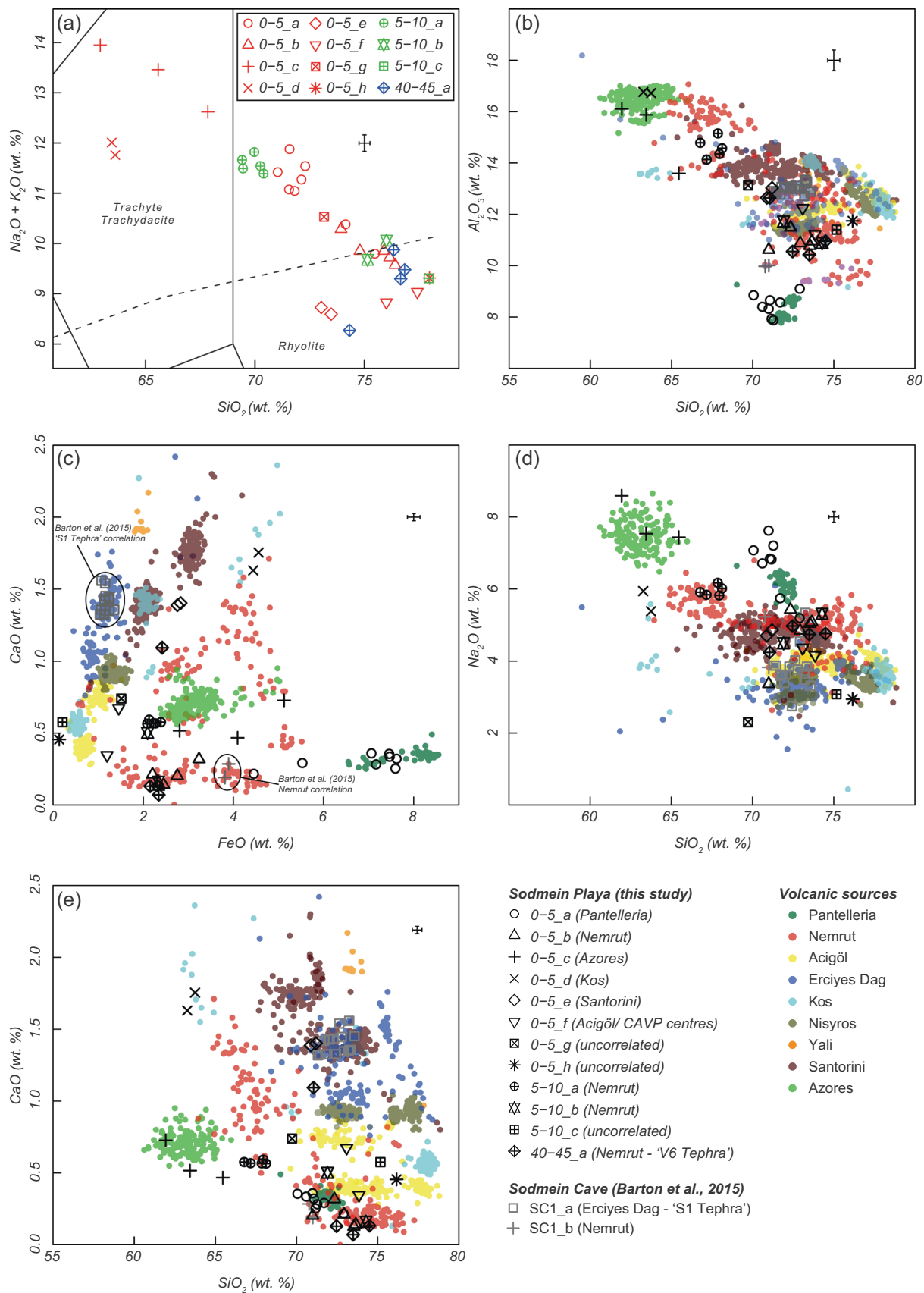


FIGURE 3 (See caption on next page)

rhyolites (population A, B, E, F, G and H) with the remaining two populations (population C and D) plotting in the trachyte field (Figure 3a; comp., BAS et al., 1986). The full suite of major element chemical data recovered from the Sodmein Playa volcanic glass shards is presented in Supporting Information: Table S1.

The single chemical population from SOD 40–45 matches most consistently with data obtained from the Nemrut volcano in the Eastern Anatolian Volcanic Province (EAVP) c. 1500 km NE of Sodmein Playa (Figure 3b–e). Nemrut is known to have been periodically active during the Holocene with at least seven eruptions spanning the period c. 7–1 ka (Macdonald et al., 2015; Schmincke & Sumita, 2014). At present, the availability of major element glass data from these eruptions is limited, thus, this correlation remains tentatively based on chemical data derived from older eruptions.

Population A and B of SOD 5–10, while clearly separable based on a number of major elements including SiO₂, Al₂O₃ and CaO wt.% totals, can both be tentatively correlated to the Nemrut volcano (Figure 3b–e). The single glass analysis comprising population C is more difficult to provenance due to its similarity to a number of known volcanic systems, namely, Kos in the Aegean and a number of centres located in the Central Anatolian Volcanic Province (CAVP) (Figure 3b–e).

The SOD 0–5 analyses provide a greater diversity of potential chemical correlatives. Population A ($n = 8$) with distinctly low Al₂O₃ wt. % values and relatively high FeO and Na₂O wt.% totals are indicative of the Pantelleria Volcano located c. 2300 km NW of Sodmein Playa (Figure 3b–d). A number of Holocene eruptions have been described from this centre with the youngest recorded activity, likely dating to c. 5–7 ka (Rotolo et al., 2021; Scaillet et al., 2011; Speranza et al., 2010). Population B ($n = 5$) is similar to SOD 40–45 and SOD 5–10 (pop B) and can thus be also tentatively correlated to Nemrut in the EAVP (Figure 3b–e). Population C ($n = 3$) matches most consistently with trachytic analyses obtained from late Holocene eruptive deposits on the Azores despite showing some minor offsets in CaO wt. % (Figure 3b–e; Johansson et al., 2017; Wastegård et al., 2020). Population D ($n = 2$) and E ($n = 2$) exhibit chemical signatures, which suggest a correlation to Kos and Santorini, respectively (Figure 3c–e). However, minor offsets in certain elements such as Al₂O₃, wt.% in regard to population D and FeO wt.% with regard to population E mean that these possible correlations are less certain. Population F ($n = 2$) exhibits similarity to Acigöl and other centres in the CAVP, although minor offsets in FeO wt.% raise some doubt (Figure 3c). Populations G ($n = 1$) and H ($n = 2$), despite showing some overlap with Nemrut and centres in the

CAVP could not be consistently correlated to a known volcanic system in the wider Mediterranean area.

5 | DISCUSSION

The results will be discussed with regard to the sedimentology and chronology, significance of cryptotephra and in terms of environmental differences compared with those of the Western Desert of Egypt.

5.1 | Sedimentological and chronological interpretation

Based on the current analyses, the previous sedimentological subdivision of the stratigraphy into four units (Kindermann et al., 2018) can now be revised to five units I–V (Figure 2). These stratigraphic units represent different types of sedimentation processes, which can be linked to climatic changes during their time of deposition in the early and mid-Holocene.

The lowermost part of the sequence consists of a thick, predominantly sandy unit, which most probably results from aeolian input into the depression. Within these sands, very fine laminae of silt but also small gravels occur, indicating only slight rainfall events and flooding of the basin (Figure 2, stratigraphic unit V). Further laminated silts (sandy silts) follow this stratigraphic unit, indicating more fluvio-lacustrine sedimentation with enhanced times of standing water during wetter climate conditions (Figure 2, stratigraphic unit IV). Stronger humid conditions, evidenced in the stratigraphy by the gradual increase in silt deposits, occur between 10 and 9 ka. This is connected to the first occurrence of laminated silts (between 70 and 90 cm), dated to the beginning of the Holocene Humid Period (PL2 9.19 ± 0.4 ka).

After the first appearance of laminated silts, indicating possible times of standing water in the depression, more dynamic flood deposits are evidenced in stratigraphic unit III. Coarse-grained sandstone fragments from the surrounding hillslopes were washed into the depression, presumably during a very dynamic climate with short but intense rainfall events. This can be associated with a drier climate in comparison to the sediment deposits below this unit. The chronology indicates that these deposits, most probably, fall into the time when the 8.2 ka event took place. This is associated with a drier climate in Northeast Africa in comparison with a wetter climate

FIGURE 3 Selected chemical plots illustrating major element glass chemistry of Sodmein Playa cryptotephra and their correlation to regional volcanic centres. Data is normalized in plot (a) (total alkali silica classification; BAS et al., 1986) and nonnormalized in biplots (b–e). Comparative chemical data from Barton et al. (2015); Cullen et al. (2014); Develle et al. (2009); Eastwood et al. (1999); Hamann et al. (2010); Karkanis et al. (2015); Macdonald et al. (2015); Margari et al. (2007); Neugebauer et al. (2021); Pe-Piper and Moulton (2008); Karaoglu et al. (2005); Satow et al. (2015); Schmincke and Sumita (2014); Schmitt et al. (2011); Şen et al. (2003); Slimak et al. (2008); Sumita and Schmincke (2013); Tomlinson et al., (2012, 2015); Tryon et al. (2009); Wastegård et al. (2020); and Wulf et al. (2018) and unpublished data from the RESET tephra database (<https://c14.arch.ox.ac.uk/>). Error bars represent 2 SD of replicate analyses ($n = 15$) of a Lipari glass standard.

before and after this phase of aridity (cf. Li et al., 2019; Thomas et al., 2007). Human occupation did not take place during the 8.2 ka event at Sodmein Cave, as climate conditions were dry and inhospitable (Vermeersch et al., 2015).

The unit is capped with thick and homogeneous, white silts with carbonates and a very compact texture. The strong increase in laminated silts and white compact silts in unit II probably indicates a phase in which the depression received more precipitation and runoff, allowing a small ephemeral lake/playa to form (Figure 2, stratigraphic unit II). It is dated to around 7.5 ka and thus coincides well with the Holocene Humid Period. This is in accordance with the archaeological results from Sodmein Cave, for which Vermeersch et al. (2015) identify human presence at the cave between 8.2–7.0 ka (6.2–5.9 ka cal. B.C., Vermeersch et al., 2015). Similarly, the wood species determination (of charcoal) from the nearby site of Tree Shelter indicates a more humid environment during this period (Marinova et al., 2008), as does sedimentological and botanical studies from fan deposits at the Gebel Duwi between 8 and 5 ka (Moeyersons et al., 1999). This is further supported by Hamdan et al. (2015), who were able to show Holocene tufa growth in the Eastern Desert between 9–10 ka and 7.2–7.0 ka. After 7 ka, the region already appears abandoned due to arid climate condition (5.0 ka cal. B.C., Vermeersch et al., 2015).

The uppermost layer (Figure 2, stratigraphic unit I) is of heterogeneous materials with mixed gravels, sand and some silt accumulations. Here, the coarse-grained gravels, comparable to stratigraphic unit III, indicate short-term runoff of water with high energy eroding the hillslopes from the surrounding Nubian Sandstone, but no further accumulation of fine silts. This indicates overall arid climate conditions after 7 ka and is consistent with the archives given above throughout the region, which also seem to support an onset of present-day hyperaridity after about 7 ka in the Eastern Desert. A strong erosion of the youngest sediments within the central depression is hard to explain, as the current wadi terraces in front of the depression and its small catchment protected the site against any larger fluvial erosion. Strong wind erosion is also unlikely due to the sheltered topographical position of the depression.

The observed mechanism of sediment accumulation can also be linked to the interpretation of the mixing of different sources of cryptotephra. The various tephra populations in the superficial layer of the profile (0–5 cm) point towards an intermixing of sediments. The low accumulation rate and the possibility that the cryptotephra are the product of secondary deposition as a result of hillslope erosion seem plausible, rather than the accumulation of primary airfall in stratigraphically distinct layers. Assuming that the eight different tephra populations were produced throughout a wider time range, their accumulation and mixing within 5 cm of sediment exclude a high input of sediments during these times. Intermixing of different cryptotephra sources in the second layer (5–10 cm) is lower than in the superficial layer. However, the described process of low sediment accumulation and in particular the deposition in a secondary context as erosional products from the hillslope must also be assumed. In contrast to this phenomenon, the third layer with notably higher glass shard concentrations at a depth of 40–45 cm represents only one

tephra population and thus is likely to represent primary aeolian deposition. Although the process of secondary depositions from erosion of the surrounding sediments in contrast to primary airfall deposition is also a possibility, higher sedimentation rates during this time result in a clearer separation of this layer. This is in good agreement with the grain-size analysis, which represents the highest number of silts, interpreted as the (relative) most humid climate conditions around 7.6 ka and thus the highest rate of sedimentation.

Unfortunately, the new dating could not confirm the previous assumption of Late Pleistocene sediments in the central depression of Sodmein Playa, as indicated by archaeological finds of the Last Interglacial from the surrounding elevated wadi terrace (Kindermann et al., 2018). In the uppermost 1.5 m of the central depression, late Pleistocene sediments were not encountered. However, the new results do not contradict the assumption that human activities at Sodmein Playa took place during the Late Pleistocene under wetter climatic conditions, since these Late Pleistocene environmental changes could be documented in the immediate vicinity by means of speleothem deposits at Saquia Cave (Henselowsky et al., 2021). Sodmein Playa is thus a distinctive case of a geoarchaeological palimpsest. The elevated area, on which the archaeological finds were made, was largely protected from erosion and has thus formed a stable surface since the Late Pleistocene. In contrast, the central depression located up to 2 m below the terrace bar was geomorphologically active and filled up with Holocene sediments. No further sediment deposition occurred on top of the elevated terrace during the Holocene. Therefore, different chronological findings occur at very short distances. Although it could not be confirmed that the lacustrine sediments of the central depression are Late Pleistocene, this does not refute the hypothesis that archaeological activities took place here in direct connection with a (temporary) lake. So far, it has not been possible to reach the sediment base of the profile in the central depression. It would therefore also be conceivable that a strong erosion of these possibly Late Pleistocene sediments has occurred.

5.2 | Tentative correlation of cryptotephra as a stratigraphic marker

The nearby Sodmein Cave provides a comparison of the tephrostratigraphic results. The primary population of the SC1 Tephra from Sodmein Cave has been correlated to the Dikkartin eruption (S1 Tephra) thought to originate from Erciyes Dag in the CAVP (Barton et al., 2015). While there is some similarity with Erciyes Dagi, other CAVP centres, and the analyses reported here, plots of FeO and CaO wt % in particular provide a clear means of discrimination between the chemistries (Figure 3c). This demonstrates that no tephra from Erciyes Dagi can be identified within the Sodmein Playa site despite the occurrence of notable ash layers such as the S1 Tephra in the wider region (e.g., Barton et al., 2015; Hamann et al., 2010; Neugebauer et al., 2021). There are, however, two analyses from the SC1 Tephra found at Sodmein Cave that seem to exhibit a

Nemrut-like chemical signature (Barton et al., 2015; Figure 3), which may therefore link with the Nemrut analyses reported here (SOD 40-45_a). The age estimate for the SC1 Tephra is 8700–9130 cal. B.P. (Neugebauer et al., 2021) and our oldest tephra at 40–45 cm is dated at around 7.61 ± 0.2 ka (Figure 2). However, based on current understanding, the earliest Holocene eruption of Nemrut (V-6) is thought to have occurred at 7192 v.y. B.P. as recorded in the Lake Van varve record (Schmincke & Sumita, 2014). Given a maximum varve counting error of 1.4% (Landmann et al., 1996), the age range for the V-6 Tephra puts it close to the age estimate of our Nemrut analyses at 40–45 cm (Figure 2; 7.61 ± 0.2 ka), but notably, not within overlapping age error estimates and too young to be a correlative of the tephra found at Sodmein Cave. This suggests that perhaps (1) the lake Van tephrostratigraphic record is incomplete and that there are earlier Holocene eruptions of Nemrut unrecognized in the proximal record; (2) our correlations and those of Barton et al. (2015) to Nemrut are incorrect and that there are other sources producing tephra of similar chemistries to Nemrut in the wider region; or (3) the occurrence of Nemrut tephra in both records is the result of reworking of older Nemrut materials deposited on the landscape before the onset of the Holocene (see Schmincke & Sumita, 2014). From the available evidence, it is not possible to definitively answer this; however, the results from distal tephra studies often lead to the revision of volcanic histories due to the sometimes-better preservation of tephra layers in distal environments compared to proximal settings (e.g., Ponomareva et al., 2015). Accepting this, it is possible that the Nemrut analyses identified in Sodmein Cave (Barton et al., 2015) correlate with those identified here at Sodmein Playa, with the apparent age inconsistencies explained by the translocation of the Nemrut glass shards at Sodmein Cave into sediments of older age and conflating with the underlying S1 Tephra. Such movement of glass shards is frequently described in cave settings owing to the complex depositional regimes operating in these settings (Barton et al., 2015; Lane et al., 2014). Finally, the sedimentation rate at Sodmein Playa (but also Sodmein Cave) is relatively low compared to higher-resolution lake sediment archives (e.g., Lake Van), with which the tephra records are compared. Ultimately there are several uncertainties associated with this proposal, but we believe that it is not beyond the realms of possibility that these two sites can be linked, albeit at this stage, tentatively.

5.3 | Transregional comparison with the Western Desert of Egypt: Similar climate, yet different environments

Besides the local importance of Sodmein Playa, and the correlation with Sodmein Cave and Tree Shelter, a transregional comparison of the climatic and environmental results with those of the Western Desert of Egypt is suggested.

Comparable playa deposits from the Djara region (Egyptian Limestone Plateau, Western Desert), located at a similar geographical latitude as Sodmein, show fast sedimentation of alternated lacustrine

and aeolian layers with a mean age of around 7.8 ka (Bubenzer & Hilgers, 2003). Thus, they seem to reflect the same chronological humid phase as the uppermost white compact silts from Sodmein Playa. Fluvio-lacustrine sediments from Abu Tartur (Western Desert) indicate rapid sedimentation of silty playa sediments with sandy layers at the beginning of the Holocene around 9.4 ka. Here, the most homogeneous playa deposits are also associated with the second wetter climate impulse during the Holocene Humid Period at around 6.23 ± 0.43 ka. In between the two phases of playa deposits, wadi sediments were deposited between 9.20 ± 0.46 and 7.16 ± 0.28 ka (Bubenzer, Besler, et al., 2007; Bubenzer, Hilgers, et al., 2007). Yet, the results from Sodmein Playa with the first impulse of wetter climate around 9 ka correlate also with the general synthesis for the Holocene occupation of the Western Desert by Kuper and Kröpelin (2006). Here, the reoccupation after the Last Glacial Maximum took place around 9 ka (8500 to 7000 B.C.E., Kuper & Kröpelin, 2006).

Even though the main climatic changes in the Eastern and the Western Desert of Egypt are comparable and thus the stratigraphy of Sodmein Playa also seems to represent the main early to mid-Holocene climate trends of Northeast Africa, important differences between these regions can be attributed with regard to the general landscape settings and the geomorphological context: similar climatic conditions do not necessarily lead to similar environmental conditions, as other aspects such as topography and geology also influence the environment and landscape in which people ultimately live.

For the sake of completeness, it should also be mentioned that the discussion of potential precipitation sources (summer rainfall vs. winter rainfall) should also be added, as discussed for example for the Fayum (cf. Phillipps et al., 2012), for Djara in the Western Desert (Kindermann et al., 2006), or for the Eastern Desert at the time of the Last Interglacial (Henselowsky et al., 2021). Evidence of Jericho Rose (*Anastatica hierochuntica*), as an indicator of Mediterranean winter rainfall, as well as Capparaceae species (*Capparis decidua* and *Maerua crassifolia*), indicating summer rainfall, were found in Djara (Kindermann et al., 2006). It can therefore be assumed that probably also the Eastern Desert, at the same latitude, has been under both winter and summer precipitation during the Holocene. In the absence of proxies to contribute to this discussion from Sodmein Playa (e.g., O-isotopes for studying the origin of precipitation), we relate the rainfall differences between the Western Desert and Eastern Desert to the landscape geomorphological context.

From a climatological perspective, the Eastern Desert should provide more environmental archives as it has turned out that this region featured, most probably due to its geographical location and its altitude, enhanced humid conditions in the past in contrast to the Western Desert (Henselowsky et al., 2021). However, the Holocene Humid Period did not create comprehensive sedimentological archives around Gebel Duwi as in comparison with the Western Desert of Egypt, where extensive archives for the Holocene climate optimum are present (Bubenzer & Riemer, 2007). The absence of these sedimentological archives is explained by the topographical and geological character of the Eastern Desert.

The dynamic and highly erosive landscape limits the preservation of (Holocene) sedimentary archives. This complex topography was already present during the Holocene. Deeply incised wadi courses lead to increased runoff with high energy in a strongly tectonic impacted region. Numerous palaeohydrological features characterize the region and there are no fundamental changes in the catchment systems for the Holocene period (Yousif et al., 2018). Thus, the potential for the creation of larger temporary/seasonal water bodies is very limited. The small morphological basins along the sandstone deposits in the western part of the Gebel Duwi are the only potential area, where playa deposition after ephemeral and/or seasonal rainfalls could have been preserved. In addition, some recent gueltas (rock pools) are known around the Gebel Duwi, but they represent a different kind of water availability, in comparison to a region with extensive paleolakes as the Western Desert of Egypt. From these different landscape contexts, the question arises of how far human activity can also be differentiated and to what extent the given landscape conditions are the cause of this.

The Holocene Humid Period with regard to human occupation is fairly well studied in the Egyptian Western Desert (e.g., Kuper & Kröpelin, 2006; Wendorf et al., 2001), whereas little is known about the Early and Middle Holocene occupation of the Eastern Desert. Comparable to the Western Desert, the Eastern Desert was not inhabited by humans during the Late Glacial Maximum (LGM) and the Early Holocene. Tree Shelter and Sodmein Cave, with their stratigraphic sequences covering a long period of time and having good preservation of organic materials, are crucial for understanding the recolonization of the area as well as the first introduction of small livestock into North Africa. After improved climatic conditions, around 9 ka, small hunter-gatherer groups returned to the Eastern Desert. Thus, the earliest occupation of Tree Shelter shows a characteristic microlithic assemblage, attributed to the Early Holocene/Epipalaeolithic (Vermeersch, 2008). The lithic inventory has similarities with the Elkabien in the Nile Valley and is interpreted by the excavators as a [...] 'succession of visits by a group of hunter-gatherers' (Vermeersch, 2008, p. 85).

The Holocene archaeozoological evidence from Sodmein Cave and Tree Shelter emphasizes that environmental conditions were different compared to the Western Desert. Huge dung deposits from goats or sheep, in Sodmein Cave as well as in Tree Shelter, indicate that the Gebel Duwi was regularly visited by herders during ecologically favourable environmental conditions.

Cattle could not be detected in the Holocene faunistic materials of Sodmein Cave, as well as of Tree Shelter, which led to the assumption [...] 'that Neolithic herds in the Eastern Desert only consisted of small livestock, and perhaps only of goat' (Vermeersch, 2008, p. 83). Linseele et al. (2010) assumed that keeping cattle was impossible in the Eastern Desert as it needs regular and more drinking water than ovicaprines.

Although livestock have been kept in the Western Desert, the different landscape context was argued to be the main reason why cattle did not occur in the Eastern Desert. Goats are much better adapted to live in arid environments and were certainly present around Gebel Duwi (Linseele et al., 2010). Our interpretation of the

Sodmein Playa sedimentary archive and the landscape context seems to confirm this assumption. There were no large lakes in the vicinity that could be used as a permanent water supply for cattle. However, this absence, in contrast to the Western Desert with larger paleolakes, cannot be traced back to a different climate. We were able to show that the general climate conditions in the Eastern Desert are comparable to those in the Western Desert of Egypt. The difference is therefore not likely to be caused by the limit of absolute water but rather by the effective water availability due to the topographic and geologic context of the Eastern Desert. This also indicates the livestock of animals that are better adapted to lower water availability.

Ultimately, therefore, an (additionally) intensified geomorphological examination of these sedimentary archives is important. They not only influence the basic existence of lakes and water in the past but also the post-sedimentary change and preservation of the sediments. These local factors and uneven preservation conditions are also conspicuous for the palaeoenvironmental reconstruction in the Western Desert (cf. Nicoll, 2004), but absolute geomorphological differences are even higher between the Eastern Desert and the Western Desert, as relative differences between sites form the Western Desert.

6 | CONCLUSION

The sedimentological sequence from Sodmein Playa is the first open-air archive of the Holocene Humid Period around the Gebel Duwi in the Egyptian Eastern Desert. The results correlate well with the archaeological investigations of the region. Around 9 ka, the sediments reveal a drier phase, which is still characterized by aeolian input but already shows clear evidence of flooding events. The beginning of the Holocene Humid Period could also be documented. Around the same time, there is evidence of human reoccupation in the area, as shown by the two nearby sites Sodmein Cave and Tree Shelter. Around 7 ka, the sediments from Sodmein Playa indicate much wetter environmental conditions, evidenced by the formation of ephemeral lake stands. This corresponds to the 'optimum' of the Holocene Humid Period for Northeast Africa, in which even remote areas were colonized and the use of domesticated sheep/goats was widespread. As evidenced by the numerous finds of this phase from Sodmein Cave and Tree Shelter, this also appears to have been the primary period of use during the Holocene in the Eastern Desert. Our observation that the relatively wettest conditions occurred after the 8.2 ka event may also be related to the settlement change at Sodmein Cave. Before the dry intermediate period of the 8.2 ka event, the conditions were wetter than during the LGM and the earliest Holocene but not as wet as after the 8.2 ka event. This supports the observation that during the first wetter phase (around 9 ka) mainly Hunter-gatherers used the region, whereas after this phase, herders regularly frequented the area (Vermeersch et al., 2015). Thus, this change in lifestyle is also possibly related to the environment. The differences in the respective livestock shown, for example,

around Tree Shelter compared with the Western Desert, also showed that environmental conditions had a decisive influence on humans. The use of goats at Tree Shelter, which is better adapted to aridity compared to cattle (Linseele et al., 2010), shows that it was still a water-limited landscape.

Overall, it can be demonstrated that similar supraregional climatological conditions (in Northeastern Africa, including the Western and Eastern Desert of Egypt) produced different regional effects, which can be related to a distinct geomorphological context and landscape setting. To understand human activity in the past, we therefore do not (only) need climate reconstructions but precisely the environmental and landscape setting, to reconstruct possible regional climatic effects and water availabilities. Sodmein Playa provides an example of a sediment archive, which at first glance appears to be poorly preserved and uninformative for a high-resolution reconstruction of climate, that can however contribute valuable insights into environmental conditions and a holistic landscape context. The possible correlation of the Nemrut-like tephra is an independent parameter to connect this timeframe from Sodmein Cave and Sodmein Playa and thus to get a direct link between an open-air and a cave site around Gebel Duwi.

Sodmein Playa demonstrates that the close interaction of morphologically active and stable surfaces determines the information content of respective geoarchaeological archives in a hyperarid landscape. An overall picture of human–environment interaction can only be obtained by considering the entire chronological depth (juxtaposition of Late Pleistocene archaeological finds and Holocene sedimentological archives), as well as the integration of other finds from the region (Tree Shelter, Sodmein Cave, Saquia Cave). However, none of the individual archives can provide a complete record of human activity in the context of environmental change during the Late Pleistocene and Holocene.

ACKNOWLEDGEMENTS

This study is part of the Collaborative Research Centre 806 'Our Way to Europe', subproject A1 'Out of Africa—Late Pleistocene Rock Shelter Stratigraphies and Palaeoenvironments in Northeast Africa', (funded grant number 57444011—SFB 806) by the Deutsche Forschungsgemeinschaft (DFG). The authors thank the Egyptian Mineral and Resources Authority (EMRA), in particular A. Almoazamy, E. Fawwez, H. Khairy and T. Khatar, for providing their help during fieldwork and sample export. Our sincere thanks go to P. Van Peer (University Leuven), who discovered Sodmein Playa, for his continuous support and collaboration. R. Timms, D. White, S. Blockley and P. Lincoln would like to thank K. Flowers and C. Hayward for their assistance with the tephra preparations and analysis. They would also like to acknowledge funding from the Leverhulme Trust as part of the 'Unravelling the pattern, impacts and drivers of early modern human dispersals from Africa' project (Grant Ref: RPG-2017-087). Open Access funding enabled and organized by Projekt DEAL.

ORCID

Felix Henselowsky  <http://orcid.org/0000-0003-4145-7958>
 Rhys Timms  <http://orcid.org/0000-0002-0894-9080>
 Paul Lincoln  <http://orcid.org/0000-0003-0566-2970>
 Simon Blockley  <http://orcid.org/0000-0003-0712-2118>
 Karin Kindermann  <http://orcid.org/0000-0003-0311-6319>
 Olaf Bubenzer  <http://orcid.org/0000-0002-3199-1156>

REFERENCES

- Ballarini, M., Wallinga, J., Wintle, A. G., & Bos, A. J. J. (2007). A modified SAR protocol for optical dating of individual grains from young quartz samples. *Radiation Measurements*, 42, 360–369. <https://doi.org/10.1016/j.radmeas.2006.12.016>
- Barton, R. N. E., Lane, C. S., Albert, P. G., White, D., Collcutt, S. N., Bouzouggar, A., Ditchfield, P., Farr, L., Oh, A., Ottolini, L., Smith, V. C., Van Peer, P., & Kindermann, K. (2015). The role of cryptotephra in refining the chronology of Late Pleistocene human evolution and cultural change in north Africa. *Quaternary Science Reviews*, 118, 151–169. <https://doi.org/10.1016/j.quascirev.2014.09.008>
- Bas, M. J. L., Maitre, R. W. L., Streckeisen, A., & Zanettin, B. (1986). A chemical classification of volcanic rocks based on the total alkali-silica diagram. *Journal of Petrology*, 27(3), 745–750. <https://doi.org/10.1093/petrology/27.3.745>
- Blockley, S. P. E., Pyne-O'Donnell, S. D. F., Lowe, J. J., Matthews, I. P., Stone, A., Pollard, A. M., Turney, C. S. M., & Molyneux, E. G. (2005). A new and less destructive laboratory procedure for the physical separation of distal glass tephra shards from sediments. *Quaternary Science Reviews*, 24(16–17), 1952–1960. <https://doi.org/10.1016/j.quascirev.2004.12.008>
- Blott, S. J., & Pye, K. (2001). GRADISTAT: A grain size distribution and statistics package for the analysis of unconsolidated sediments. *Earth Surface Processes and Landforms*, 26, 1237–1248. <https://doi.org/10.1002/esp.261>
- Brennan, B. J. (2003). Beta doses to spherical grains. *Radiation Measurements*, 37, 299–303. [https://doi.org/10.1016/S1350-4487\(03\)00011-8](https://doi.org/10.1016/S1350-4487(03)00011-8)
- Brennan, B. J., Lyons, R. G., & Phillips, S. W. (1991). Attenuation of alpha particle track dose for spherical grains. *International Journal of Radiation Applications and Instrumentation. Part D. Nuclear Tracks and Radiation Measurements*, 18, 249–253. [https://doi.org/10.1016/1359-0189\(91\)90119-3](https://doi.org/10.1016/1359-0189(91)90119-3)
- Bubenzer, O., Besler, H., & Hilgers, A. (2007). Filling the gap: OSL data expanding ¹⁴C Chronologies of Late Quaternary environmental change in the Libyan Desert. *Quaternary International*, 175, 41–52. <https://doi.org/10.1016/j.quaint.2007.03.014>
- Bubenzer, O., & Hilgers, A. (2003). Luminescence dating of Holocene playa sediments of the Egyptian Plateau Western Desert, Egypt. *Quaternary Science Reviews*, 22, 1077–1084. [https://doi.org/10.1016/S0277-3791\(03\)00061-1](https://doi.org/10.1016/S0277-3791(03)00061-1)
- Bubenzer, O., Hilgers, A., & Riemer, H. (2007). Luminescence dating and archaeology of Holocene fluvio-lacustrine sediments of Abu Tartur, Eastern Sahara. *Quaternary Geochronology*, 2(1–4), 314–321. <https://doi.org/10.1016/j.quageo.2006.04.014>
- Bubenzer, O., & Riemer, H. (2007). Holocene climatic change and human settlement between the Central Sahara and the Nile Valley: Archaeological and geomorphological results. *Geoarchaeology*, 22(6), 607–620. <https://doi.org/10.1002/gea.20176>
- Cullen, V. L., Smith, V. C., & Arz, H. W. (2014). The detailed tephrostratigraphy of a core from the south-east Black Sea spanning the last ~60 ka. *Journal of Quaternary Science*, 29(7), 675–690. <https://doi.org/10.1002/jqs.2739>
- Cunningham, A. C., & Wallinga, J. (2010). Selection of integration time intervals for quartz OSL decay curves. *Quaternary Geochronology*, 5, 657–666. <https://doi.org/10.1016/j.quageo.2010.08.004>

- Develle, A. L., Williamson, D., Gasse, F., & Walter-Simonnet, A. V. (2009). Early Holocene volcanic ash fallout in the Yammoûneh lacustrine basin (Lebanon): Tephrochronological implications for the Near East. *Journal of Volcanology and Geothermal Research*, 186(3–4), 416–425. <https://doi.org/10.1016/j.jvolgeores.2009.07.016>
- Duller, G. A. T. (2003). Distinguishing quartz and feldspar in single grain luminescence measurements. *Radiation Measurements*, 37, 161–165. [https://doi.org/10.1016/S1350-4487\(02\)00170-1](https://doi.org/10.1016/S1350-4487(02)00170-1)
- Durcan, J. A., King, G. E., & Duller, G. A. T. (2015). DRAC: Dose rate and age calculator for trapped charge dating. *Quaternary Geochronology*, 28, 54–61. <https://doi.org/10.1016/j.quageo.2015.03.012>
- Eastwood, W. J., Pearce, N. J. G., Westgate, J. A., Perkins, W. T., Lamb, H. F., & Roberts, N. (1999). Geochemistry of Santorini tephra in lake sediments from Southwest Turkey. *Global and Planetary Change*, 21(1–3), 17–29. [https://doi.org/10.1016/S0921-8181\(99\)00005-3](https://doi.org/10.1016/S0921-8181(99)00005-3)
- Guerin, G., Mercier, N., & Adamiec, G. (2011). Dose-rate conversion factors: Update. *Anc. TL*, 29, 5–8.
- Hamann, Y., Wulf, S., Ersoy, O., Ehrmann, W., Aydar, E., & Schmiedl, G. (2010). First evidence of a distal early Holocene ash layer in Eastern Mediterranean deep-sea sediments derived from the Anatolian volcanic province. *Quaternary Research*, 73(3), 497–506. <https://doi.org/10.1016/j.yqres.2009.12.004>
- Hamdan, M. A., & Brook, G. A. (2015). Timing and characteristics of Late Pleistocene and Holocene wetter periods in the Eastern Desert and Sinai of Egypt, based on ¹⁴C dating and stable isotope analysis of spring tufa deposits. *Quaternary Science Reviews*, 130, 168–188. <https://doi.org/10.1016/j.quascirev.2015.09.011>
- Hayward, C. (2012). High spatial resolution electron probe microanalysis of tephra and melt inclusions without beam-induced chemical modification. *The Holocene*, 22(1), 119–125. <https://doi.org/10.1177/0959683611409777>
- Henselowsky, F., Eichstädter, R., Schröder-Ritzrau, A., Herwartz, D., Almoazamy, A., Frank, N., Kindermann, K., & Bubenzer, O. (2021). Speleothem growth phases in the central Eastern Desert of Egypt reveal enhanced humidity throughout MIS 5. *Quaternary International*. <https://doi.org/10.1016/j.quaint.2021.05.006>
- Hunt, J. B., & Hill, P. G. (1993). Tephra geochemistry: A discussion of some persistent analytical problems. *The Holocene*, 3, 271–278. <https://doi.org/10.1177/095968369300300310>
- Johansson, H., Lind, E. M., & Wastegård, S. (2017). Compositions of glass in proximal tephra from eruptions in the Azores archipelago and their links with distal sites in Ireland. *Quaternary Geochronology*, 40, 120–128. <https://doi.org/10.1016/j.quageo.2016.07.006>
- Karaoglu, O., Ozdemir, Y., Tolluoglu, A. U., Karabiyikoglu, M., Kose, O., & Froger, J.-L. (2005). Stratigraphy of the volcanic products around Nemrut caldera: Implications for reconstruction of the caldera formation. *Turkish Journal of Earth Sciences*, 14(2), 123–143.
- Karkanis, P., White, D., Lane, C. S., Stringer, C., Davies, W., Cullen, V. L., Smith, V. C., Ntinou, M., Tsartsidou, G., & Kyparissi-Apostolika, N. (2015). Tephra correlations and climatic events between the MIS6/5 transition and the beginning of MIS3 in Theopetra Cave, central Greece. *Quaternary Science Reviews*, 118, 170–181. <https://doi.org/10.1016/j.quascirev.2014.05.027>
- Kindermann, K., Bubenzer, O., Nussbaum, S., Riemer, H., Darius, F., Pöllath, N., & Smettan, U. (2006). Palaeoenvironment and Holocene land use of Djara, Western Desert of Egypt. *Quaternary Science Reviews*, 25, 1619–1637. <https://doi.org/10.1016/j.quascirev.2005.12.005>
- Kindermann, K., Van Peer, P., & Henselowsky, F. (2018). At the lakeshore—An early Nubian complex site linked with lacustrine sediments (Eastern Desert, Egypt). *Quaternary International*, 485, 131–139. <https://doi.org/10.1016/j.quaint.2017.11.006>
- Klasen, N., Kehl, M., Mikdad, A., Brückner, H., & Weniger, G. -C. (2018). Chronology and formation processes of the Middle to Upper Palaeolithic deposits of Ifri n'Ammar using multi-method luminescence dating and micromorphology. *Quaternary International*, 485, 89–102. <https://doi.org/10.1016/j.quaint.2017.10.043>
- Kuper, R., & Kröpelin, S. (2006). Climate-controlled Holocene occupation in the Sahara: Motor of Africa's evolution. *Science*, 313(803), 803–807. <https://doi.org/10.1126/science.1130989>
- Landmann, G., Reimer, A., & Kempe, S. (1996). Climatically induced lake level changes at Lake Van, Turkey, during the Pleistocene/Holocene transition. *Global Biogeochemical Cycles*, 10(4), 797–808. <https://doi.org/10.1029/96GB02347>
- Lane, C. S., Cullen, V. L., White, D., Bramham-Law, C. W. F., & Smith, V. C. (2014). Cryptotephra as a dating and correlation tool in archaeology. *Journal of Archaeological Science*, 42, 42–50.
- Li, H., Renssen, H., Roche, D. M., & Miller, P. A. (2019). Modelling the vegetation response to the 8.2 ka BP cooling event in Europe and Northern Africa. *Journal of Quaternary Science*, 34(8), 650–661. <https://doi.org/10.1002/jqs.3157>
- Linseele, V., Marinova, E., Van Neer, W., & Vermeersch, P. M. (2010). Sites with Holocene dung deposits in the Eastern Desert of Egypt: Visited by herders. *Journal of Arid Environments*, 74, 818–828. <https://doi.org/10.1016/j.jaridenv.2009.04.014>
- Litt, T., Richter, J., & Schäbitz, F. (2021). *The journey of modern humans from Africa to Europe. Culture environmental interaction and mobility* (p. 372). Schweizerbart.
- Macdonald, R., Sumita, M., Schmincke, H. U., Bagiński, B., White, J. C., & Ilnicki, S. S. (2015). Peralkaline felsic magmatism at the Nemrut volcano, Turkey: impact of volcanism on the evolution of Lake Van (Anatolia) IV. *Contributions to Mineralogy and Petrology*, 169(4), 34. <https://doi.org/10.1007/s00410-015-1127-6>
- Margari, V., Pyle, D. M., Bryant, C., & Gibbard, P. L. (2007). Mediterranean tephra stratigraphy revisited: results from a long terrestrial sequence on Lesvos Island, Greece. *Journal of Volcanology and Geothermal Research*, 163(1–4), 34–54. <https://doi.org/10.1016/j.jvolgeores.2007.02.002>
- Marinova, E., Linseele, V., & Vermeersch, P. (2008). Holocene environment and subsistence patterns near the tree shelter, Red Sea Mountains, Egypt. *Quaternary Research*, 70, 392–397. <https://doi.org/10.1016/j.yqres.2008.08.002>
- Moeyersons, J., Vermeersch, P. M., Beeckman, H., & Van Peer, P. (1999). Holocene environmental changes in the Gebel Umm Hammad, Eastern Desert, Egypt. *Geomorphology*, 26, 297–312. [https://doi.org/10.1016/S0169-555X\(98\)00067-1](https://doi.org/10.1016/S0169-555X(98)00067-1)
- Murray, A. S., & Wintle, A. G. (2000). Luminescence dating of quartz using an improved single-aliquot regenerative-dose protocol. *Radiation Measurements*, 32, 57–73. [https://doi.org/10.1016/S1350-4487\(99\)00253-X](https://doi.org/10.1016/S1350-4487(99)00253-X)
- Murray, A. S., & Wintle, A. G. (2003). The single aliquot regenerative dose protocol: Potential for improvements in reliability. *Radiation Measurements*, 37, 377–381. [https://doi.org/10.1016/S1350-4487\(03\)00053-2](https://doi.org/10.1016/S1350-4487(03)00053-2)
- Neugebauer, I., Müller, D., Schwab, M. J., Blockley, S., Lane, C. S., Wulf, S., Appelt, O., & Brauer, A. (2021). Cryptotephra in the Lateglacial ICDP Dead Sea sediment record and their implications for chronology. *Boreas*, 50(3), 844–861. <https://doi.org/10.1111/bor.12516>
- Nicoll, K. (2004). Recent environmental change and prehistoric human activity in Egypt and Northern Sudan. *Quaternary Science Reviews*, 23, 561–580. <https://doi.org/10.1016/j.quascirev.2003.10.004>
- Van Peer, P., Vermeersch, P., Moeyersons, J., & Van Neer, W. (1996). Palaeolithic sequence of Sodmein cave, red Sea Mountains, Egypt. In G. Pwiti, & R. Soper (Eds.), *Aspects of African Archaeology Papers from the 10th Congress of the Panafrikan Association for Prehistory and Related Studies* (pp. 149–156). Harare.
- Pe-Piper, G., & Moulton, B. (2008). Magma evolution in the Pliocene–Pleistocene succession of Kos, South Aegean arc (Greece). *Lithos*, 106(3), 110–124. <https://doi.org/10.1016/j.lithos.2008.07.002>

- Phillipps, R., Holdaway, S., Wendrich, W., & Cappers, R. (2012). Mid-Holocene occupation of Egypt and global climatic change. *Quaternary International*, 251, 64–76. <https://doi.org/10.1016/j.quaint.2011.04.004>
- Ponomareva, V., Portnyagin, M., & Davies, S. M. (2015). Tephra without borders: Far-reaching clues into past explosive eruptions. *Frontiers in Earth Science*, 3, 83.
- Prescott, J. R., & Hutton, J. T. (1994). Cosmic ray contributions to dose rates for luminescence and ESR dating: Large depths and long-term time variations. *Radiation Measurements*, 23(2–3), 497–500. [https://doi.org/10.1016/1350-4487\(94\)90086-8](https://doi.org/10.1016/1350-4487(94)90086-8)
- Richter, J., Melles, M., & Schäbitz, F. (2012). Temporal and spatial corridors of *Homo sapiens sapiens* population dynamics during the Late Pleistocene and early Holocene. *Quaternary International*, 274, 1–4. <https://doi.org/10.1016/j.quaint.2012.06.009>
- Rotolo, S. G., Scaillet, S., Speranza, F., White, J. C., Williams, R., & Jordan, N. J. (2021). Volcanological evolution of Pantelleria Island (Strait of Sicily) peralkaline volcano: A review. *Comptes Rendus. Géoscience*, 353(S2), 111–132. <https://doi.org/10.5802/crgeos.51>
- Satow, C., Tomlinson, E. L., Grant, K. M., Albert, P. G., Smith, V. C., Manning, C. J., Ottoloni, L., Wulf, S., Rohling, E. J., Lowe, J. J., Blockley, S. P. E., & Menzies, M. A. (2015). A new contribution to the Late Quaternary tephrostratigraphy of the Mediterranean: Aegean Sea core LC21. *Quaternary Science Reviews*, 117, 96–112. <https://doi.org/10.1016/j.quascirev.2015.04.005>
- Scaillet, S., Rotolo, S. G., La Felice, S., & Vita-Scaillet, G. (2011). High-resolution ⁴⁰Ar/³⁹Ar chronostratigraphy of the post-caldera (<20 ka) volcanic activity at Pantelleria, Sicily Strait. *Earth and Planetary Science Letters*, 309(3–4), 280–290. <https://doi.org/10.1016/j.epsl.2011.07.009>
- Schmidt, C., Kindermann, K., Van Peer, P., & Bubenzer, O. (2015). Multi-emission luminescence dating of heated chert from the Middle Stone Age sequence at Sodmein Cave (Red Sea Mountains, Egypt). *Journal of Archaeological Science*, 63, 94–103. <https://doi.org/10.1016/j.jas.2015.08.016>
- Schmincke, H. U., & Sumita, M. (2014). Impact of volcanism on the evolution of Lake Van (eastern Anatolia) III: Periodic (Nemrut) vs. episodic (Süphan) explosive eruptions and climate forcing reflected in a tephra gap between ca. 14 ka and ca. 30 ka. *Journal of Volcanology and Geothermal Research*, 285, 195–213. <https://doi.org/10.1016/j.jvolgeores.2014.08.015>
- Schmitt, A. K., Danišik, M., Evans, N. J., Siebel, W., Kiemle, E., Aydin, F., & Harvey, J. C. (2011). Acigöl rhyolite field, Central Anatolia (part 1): High-resolution dating of eruption episodes and zircon growth rates. *Contributions to Mineralogy and Petrology*, 162(6), 1215–1231. <https://doi.org/10.1007/s00410-011-0648-x>
- Şen, E., Kürkcüoğlu, B., Aydar, E., Gourgaud, A., & Vincent, P. M. (2003). Volcanological evolution of Mount Erciyes stratovolcano and origin of the Valibaba Tepe ignimbrite (Central Anatolia, Turkey). *Journal of Volcanology and Geothermal Research*, 125(3), 225–246. [https://doi.org/10.1016/S0377-0273\(03\)00110-0](https://doi.org/10.1016/S0377-0273(03)00110-0)
- Slimak, L., Kuhn, S. L., Roche, H., Muralis, D., Buitenhuis, H., Balkan-Atli, N., Binder, D., Kuzucuoğlu, C., & Guillou, H. (2008). Kaletepe Deresi 3 (Turkey): Archaeological evidence for early human settlement in Central Anatolia. *Journal of Human Evolution*, 54(1), 99–111. <https://doi.org/10.1016/j.jhevol.2007.07.004>
- Speranza, F., Landi, P., D'Ajello Caracciolo, F., & Pignatelli, A. (2010). Paleomagnetic dating of the most recent silicic eruptive activity at Pantelleria (Strait of Sicily). *Bulletin of Volcanology*, 72(7), 847–858. <https://doi.org/10.1007/s00445-010-0368-5>
- Sumita, M., & Schmincke, H. U. (2013). Impact of volcanism on the evolution of Lake Van I: Evolution of explosive volcanism of Nemrut Volcano (eastern Anatolia) during the past >400,000 years. *Bulletin of Volcanology*, 75(5), 714. <https://doi.org/10.1007/s00445-013-0714-5>
- Thomas, E. R., Wolff, E. W., Mulvaney, R., Steffensen, J. P., Johnsen, S. J., Arrowsmith, C., White, J. W. C., Vaughn, B., & Popp, T. (2007). The 8.2 ka event from Greenland ice cores. *Quaternary Science Reviews*, 26, 70–81. <https://doi.org/10.1016/j.quascirev.2006.07.017>
- Tomlinson, E. L., Kinvis, H. S., Smith, V. C., Blundy, J. D., Gottsmann, J., Müller, W., & Menzies, M. A. (2012). The Upper and Lower Nisyros Pumices: Revisions to the Mediterranean tephrostratigraphic record based on micron-beam glass geochemistry. *Journal of Volcanology and Geothermal Research*, 243–244, 69–80. <https://doi.org/10.1016/j.jvolgeores.2012.07.004>
- Tomlinson, E. L., Smith, V. C., Albert, P. G., Aydar, E., Civetta, L., Cioni, R., Çubukçu, E., Gertisser, R., Isaia, R., Menzies, M. A., Orsi, G., Rosi, M., & Zanchetta, G. (2015). The major and trace element glass compositions of the productive Mediterranean volcanic sources: Tools for correlating distal tephra layers in and around Europe. *Quaternary Science Reviews*, 118, 48–66. <https://doi.org/10.1016/j.quascirev.2014.10.028>
- Tryon, C. A., Logan, M. A. V., Muralis, D., Kuhn, S., Slimak, L., & Balkan-Atli, N. (2009). Building a tephrostratigraphic framework for the Paleolithic of central Anatolia, Turkey. *Journal of Archaeological Science*, 36(3), 637–652. <https://doi.org/10.1016/j.jas.2008.10.006>
- Vermeersch, P. M. (2008). *A Holocene prehistoric sequence in the Egyptian Red Sea area: The tree shelter*. Egyptian Prehistory Monographs 7.
- Vermeersch, P. M., Linseele, V., Marinova, E., Van Neer, W., Moeyersons, J., & Rethemeyer, J. (2015). Early and middle Holocene human occupation of the Egyptian Eastern Desert: Sodmein cave. *African Archaeological Review*, 32, 465–503. <https://doi.org/10.1007/s10437-015-9195-6>
- Wastegård, S., Johansson, H., & Pacheco, J. M. (2020). New major element analyses of proximal tephra from the Azores and suggested correlations with cryptotephra in North-West Europe. *Journal of Quaternary Science*, 35(1–2), 114–121. <https://doi.org/10.1002/jqs.3155>
- Wendorf, F., Schild, R., & Associates. (2001). *Holocene settlement of the Egyptian Sahara, The archaeology of Nabta Playa* (Vol. 1). Kluwer Academic/Plenum Publishers.
- Wulf, S., Hardiman, M. J., Staff, R. A., Koutsodendris, A., Appelt, O., Blockley, S. P. E., Lowe, J. J., Manning, C. J., Ottoloni, L., Schmitt, A. K., Smith, V. C., Tomlinson, E. L., Vakhrameeva, P., Knipping, M., Kotthoff, U., Milner, A. M., Müller, U. C., Christianis, K., Kalaitzidis, S., ... Pross, J. (2018). The marine isotope stage 1–5 cryptotephra record of Tenaghi Philippon, Greece: Towards a detailed tephrostratigraphic framework for the Eastern Mediterranean region. *Quaternary Science Reviews*, 186, 236–262. <https://doi.org/10.1016/j.quascirev.2018.03.011>
- Yousif, M., Henselowsky, F., & Bubenzer, O. (2018). Palaeohydrology and its impact on groundwater in arid environments: Gebel Duwi and its vicinities, Eastern Desert, Egypt. *Catena*, 171, 29–43. <https://doi.org/10.1016/j.catena.2018.06.028>

SUPPORTING INFORMATION

Additional supporting information can be found online in the Supporting Information section at the end of this article.

How to cite this article: Henselowsky, F., Klasen, N., Timms, R., White, D., Lincoln, P., Blockley, S., Kindermann, K., & Bubenzer, O. (2023). Rare Holocene sediment deposits from Sodmein Playa (Eastern Desert, Egypt)—Stratigraphic assessment and environmental setting. *Geochronology*, 38, 186–198. <https://doi.org/10.1002/gea.21946>